Available online at www.sciencedirect.com

ScienceDirect

Developmental Biology 307 (2007) 152–164

DEVELOPMENTAL BIOLOGY

www.elsevier.com/locate/ydbio

Xenopus Bicaudal-C is required for the differentiation of the amphibian pronephros

Uyen Tran, L. Mary Pickney, B. Duygu Özpolat, Oliver Wessely *

LSU Health Sciences Center, Departments of Cell Biology & Anatomy and Genetics, MEB-6A12, 1901 Perdido Street, New Orleans, LA 70112, USA

Received for publication 2 February 2007; revised 18 April 2007; accepted 24 April 2007
Available online 1 May 2007

Abstract

The RNA-binding molecule Bicaudal-C regulates embryonic development in *Drosophila* and *Xenopus*. Interestingly, mouse mutants of Bicaudal-C do not show early patterning defects, but instead develop polycystic kidney disease (PKD). To further investigate the molecular mechanism of Bicaudal-C in kidney development, we analyzed its function in the developing amphibian pronephros. *Bicaudal-C* mRNA was present in the epithelial structures of the *Xenopus* pronephros, the tubules and the duct, but not the glomus. Inhibition of the translation of endogenous Bicaudal-C with antisense morpholino oligomers (*xBic-C-MO*) led to a PKD-like phenotype in *Xenopus*. Embryos lacking Bicaudal-C developed generalized edemas and dilated pronephric tubules and ducts. This phenotype was caused by impaired differentiation of the pronephros. Molecular markers specifically expressed in the late distal tubule were absent in *xBic-C-MO*-injected embryos. Furthermore, Bicaudal-C was not required for primary cilia formation, an important organelle affected in PKD. These data support the idea that Bicaudal-C functions downstream or parallel of a cilia-regulated signaling pathway. This pathway is required for terminal differentiation of the late distal tubule of the *Xenopus* pronephros and regulates renal epithelial cell differentiation, which – when disrupted – results in PKD.

Keywords: ARPKD; ADPKD; Bicaudal-C; *bpk*; Cilia; Edema; *jcpk*; Kidney; Polaris; Pronephros; *Xenopus*

Introduction

The vertebrate kidney is a complex organ used to remove metabolic waste products from the body and to conserve water, essential electrolytes and metabolites. During kidney development three successive renal structures of increasing complexity, the pro-, meso- and metanephros, form from the intermediate mesoderm via inductive processes (Saxén, 1987; Vize et al., 2002). The nephron is the structural and functional unit for each of these three kidney types and the differences lie in the amount of the individual nephrons and their organization within the kidney. Among the three kidney forms, the pronephros is the first functional kidney in amphibians and fish. It is a much simpler organ than the meso- or metanephric kidney and is only present as a rudiment in higher vertebrates. It consists of three main components, the blood-filtering glomus/glomerulus, the pronephric tubules and the pronephric duct, which transports the wastes to the cloaca (Fig. 1D). Interestingly, the genetic programs regulating kidney formation are evolutionarily conserved in all vertebrates (Carroll and McMahon, 2003; Jones, 2003). Cell-type-specific transcription factors show similar expression patterns in *Xenopus*, fish, mice and humans. The simplicity of the pronephros has made it an attractive model to study the early events in kidney development, but has also received attention in the study of kidney diseases (Drummond, 2005; Jones, 2005). In particular, the zebrafish pronephric kidney has been extensively used to study polycystic kidney disease (Drummond et al., 1998; Liu et al., 2002; Otto et al., 2003; Sun et al., 2004; Obara et al., 2006).

Polycystic kidney diseases (PKD) are characterized by the presence of renal cysts, fluid-filled epithelial-lined cavities, arising from the glomerulus, the renal tubules or the collecting ducts. While single cysts are common and relatively benign, structural abnormalities seen in clinical practice, over 70 distinct syndromes are associated with renal cysts. Among these, PKDs are the leading causes of end-stage renal disease in children and adults. Autosomal-dominant polycystic kidney

* Corresponding author. Fax: +1 504 568 4392.
E-mail address: owesse@lsuhsc.edu (O. Wessely).

0012-1606/$ - see front matter © 2007 Elsevier Inc. All rights reserved.
doi:10.1016/j.ydbio.2007.04.030

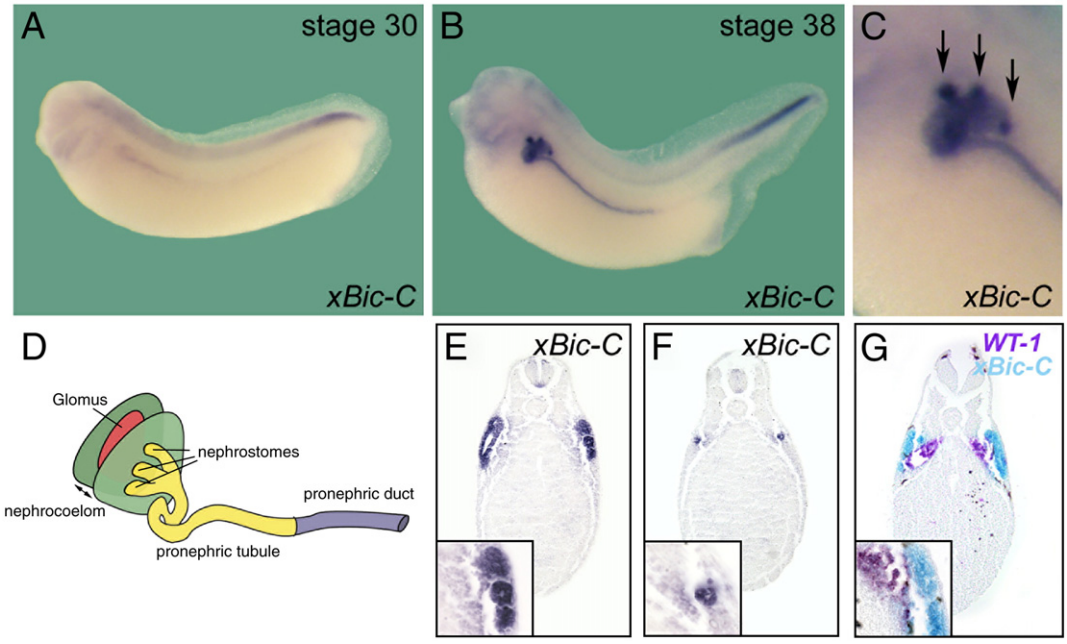

Fig. 1. Pronephros expression of *xBic-C*. (A–C) Whole mount *in situ* hybridization analysis of *xBic-C* at (A) stage 30 and (B) stage 38 showing expression in the pronephric tubules and duct. (C) Close up of B; arrows indicate the expression of *Bicaudal-C* in the three nephrostomes. (D) Schematic diagram of the amphibian pronephros. (E, F) Anterior and posterior transverse section of (B) showing *xBic-C* expression in the tubules and duct, respectively. (G) Double *in situ* hybridization with *WT-1* (purple) and *xBic-C* (turquoise). Note that *xBic-C* is expressed only in the epithelial components of the pronephros, whereas *WT-1* is expressed specifically in the glomus. Inserts in E–G are close-ups of the pronephric region highlighting the epithelium-specific expression of *Bicaudal-C*.

disease (ADPKD) is one of the most common single gene disorders in humans, affecting 1 in 800 individuals in the United States. It is characterized by massive cystic enlargement affecting all tubular segments of both kidneys. It primarily occurs as a result of mutations in two genes, *Pkd1* and *Pkd2*, which encode polycystin-1 and polycystin-2. Polycystin-1 is a membrane mechanoreceptor-like protein that forms multiprotein complexes at focal adhesions, cell–cell junctions, and cilia (Hughes et al., 1995). Polycystin-2 is a calcium-permeable cation channel that interacts with the polycystin-1 complex (Mochizuki et al., 1996). A second type of PKD, autosomal-recessive polycystic kidney disease (ARPKD), is less frequent (1 in 20,000), but often causes fetal or neonatal death due to bilateral kidney enlargement, impaired lung development, and pulmonary hypoplasia. ARPKD is primarily caused by mutations in a single gene, *PKHD1*, which encodes the receptor-like membrane protein Polyductin/Fibrocystin (Hildebrandt et al., 1997; Ward et al., 2002).

The pathobiology of PKD is still poorly understood at the cellular and molecular level. However, most of the proteins involved in PKD are localized to the proximity of primary cilia (Barr et al., 2001; Yoder et al., 2002a; Ward et al., 2003). Primary cilia are found on the apical cell surface of all renal epithelial cells except intercalated cells (Pfaller and Klima, 1976). They are characterized by 9 peripheral doublets of microtubules, but lack the central microtubule pair (9+0 pattern) present in motile cilia (9+2 pattern). Most primary cilia are immotile and have been thought to be vestigial. Emerging evidence now suggests that primary cilia function as mechanosensors of luminal flow (Nauli et al., 2003). Upon stimulation they trigger the release of intracellular calcium, which in turn regulates proliferation and differentiation of kidney epithelial cells. It has been suggested that mutations in PKD genes lead to cilia dysfunction. Interestingly, primary motile cilia have also been detected in the node of mouse and the corresponding organs of other vertebrates, where they regulate left–right patterning (Essner et al., 2002; McGrath et al., 2003; Kramer-Zucker et al., 2005; Shiratori and Hamada, 2006; Schweickert et al., 2007).

Many mouse and rat models of PKD share the common pathogenic features of the human disease such as dysregulation of epithelial cell proliferation and differentiation, changes in the extracellular matrix, and abnormalities in epithelial cell polarity and transepithelial fluid transport (Guay-Woodford, 2003). Recently, two of these PKD mouse models, *bpk* and *jcpk*, have been shown to result from mutations in a single gene, *Bicaudal-C* (Cogswell et al., 2003). The BALB/c polycystic kidney (*bpk*) mutation arose spontaneously and resembles ARPKD. The homozygous mice die at 4 weeks of age due to renal insufficiency and display cystic dilatations of the renal collecting duct and biliary dysgenesis (Nauta et al., 1993). The juvenile congenital polycystic kidney (*jcpk*) mutation was identified in the course of a chlorambucil mutagenesis screen (Flaherty et al., 1995). Homozygous *jcpk* mutant mice die before 10 days of age and have numerous cysts in all parts of the nephron, including the proximal and distal tubules, collecting ducts and glomeruli.

Bicaudal-C was originally identified in a *Drosophila* mutagenesis screen, as a gene in which heterozygous females produced embryos with “double-abdomen” phenotypes (Mohler and Wieschaus, 1986). *Bicaudal-C* encodes an RNA-binding

molecule, consisting of 5 amino-terminal KH (hnRNP *K Homology*) RNA-binding domains and a C-terminal protein–protein interaction SAM (Sterile Alpha Motif) domain. We identified the *Xenopus* homologue of *Bicaudal-C* in the course of a screen for genes regulating early amphibian development (Wessely and De Robertis, 2000). Whole mount *in situ* hybridization showed early expression of *Bicaudal-C* in the vegetal half of the *Xenopus* egg, later in the dorsal blastopore lip of the late gastrula and finally in the neural tube and the developing pronephros at tailbud stage. The mouse homologue of Bicaudal-C is expressed in the same, as well as additional embryonic territories (Wessely et al., 2001). Microinjection of synthetic *Bicaudal-C* mRNA into *Xenopus* embryos induced ectopic endoderm formation and this activity required the KH RNA-binding domains of Bicaudal-C, but not the SAM protein–protein interaction domain. These data led to the hypothesis that Bicaudal-C acts as an endodermal determinant regulating germ layer patterning (Wessely and De Robertis, 2000).

Here, we analyzed the function of Bicaudal-C in *Xenopus* pronephros development. *xBic-C* is expressed in the renal epithelial cells of the amphibian pro- and mesonephros. Microinjection of antisense morpholino oligomers against xBic-C resulted in dilated pronephric tubules and edema formation, likely as a result of impaired water and solute homeostasis. This phenotype was not caused by early defects in pronephric development, but rather by impaired differentiation of the late distal tubule and pronephric duct. Moreover, we also observed defects in left–right patterning, suggesting an important role for Bicaudal-C in cilia-regulated signaling.

Materials and methods

Embryo manipulations

Xenopus embryos obtained by *in vitro* fertilization were maintained in 0.1× modified Barth medium (Sive et al., 2000) and staged according to Nieuwkoop and Faber (1994). The sequences of the antisense morpholino oligomers used in this study were 5′-TAG ACT CGC ACT GAG CCG CCA TTC T-3′ (*xBic-C-MO1*), 5′-CCA TTG TGC TAC TGC CGC CGC TAA C-3′ (*xBic-C-MO2*), 5′-CGA TTC TGC TAG TGC GGC CCC TAA C-3′ (*xBic-C-MO2*-scrambled) and 5′-GGC ACG AGA TGG ACA TTT TGC ATC A-3′ (*xPol-MO*). Antisense morpholino oligomers were diluted to a concentration of 1 mM. *xBic-C-MO1*, *xBicC-MO-2* were used at a final concentration of 125 μM or 250 μM, *xBic-C-MO1+2* as the mixture of 125 μM *xBic-C-MO1* and 125 μM *xBic-C-MO2*, the standard control morpholino oligomer and *xBicC-MO2-scrambled* at 125 μM and *xPol-MO* at a concentration 100 μM. For all the injections a total of 8 nl of morpholino oligomer solution was injected radially at the 2- to 4-cell stage into *Xenopus* embryos. *pCS2-xBic-C** was generated by PCR mutagenesis introducing eight nucleotide changes, so that the construct was no longer targeted by the Bicaudal-C antisense morpholino oligomers, but was translated into a protein with identical amino acid sequence. *pCS2-Polaris* was sub-cloned from *pSK-polaris* (GenBank Accession Number: BJ051594) using *Eco*RI and *Xho*I; *pCS2-xBic-C-ΔKH* and *pCS2-xBic-C-ΔSAM* were described previously (Wessely and De Robertis, 2000). For synthetic mRNA all plasmids were linearized with *Not*I and transcribed with SP6 RNA polymerase using the mMessage mMachine® (Ambion).

Whole mount in situ hybridizations

Whole mount *in situ* hybridizations were performed as described at http://www.hhmi.ucla.edu/derobertis. To generate antisense probes the plasmids were linearized and transcribed as follows: *pSK-Axonemal Dynein Heavy Chain 9* (GenBank Accession Number: BJ084882) –*Eco*RI/T7, *pSK-xBicC* (Wessely and De Robertis, 2000) – *Not*I/T7, *pGEM®-T-Easy-Carbonic Anhydrase II* – *Pst*I/T7, *pBC-ClC-K* (Vize, 2003) – *Eco*RI/T7, *pCMV-SPORT6-FoxJ1* (GenBank Accession Number: CA791310) – *Sal*I/T7, *pSK-GATA3* (GenBank Accession Number: BJ067977) – *Eco*RI/T7, *pGEM-T-HNF1β* (Vignali et al., 2000) – *Asp718*/T7, *pCS105-Lefty* (GenBank Accession Number: BP693306) – *Bam*HI/T7, *pSP64TS-Lim-1* (Carroll et al., 1999) – *Xho*I/T7, *pSK*-β1-Na-K-ATPase (GenBank Accession Number: BJ077182) – *Eco*RI/T7, *pCMV-SPORT6-xNBC1* (Zhou and Vize, 2004) – *Sal*I/T7, *pSK-NCC2* (GenBank Accession Number: BJ076552) – *Eco*RI/T7, *pCMV-SPORT6-Nephrin* (GenBank Accession Number: BI477611) – *Eco*RI/T7, pSK-NKCC2 (GenBank Accession Number: BJ037567) – *Sma*I/T7, *pSK-Pax-2* (Carroll et al., 1999) – *Xba*I/T7, *pSK-Pax-8* (Carroll et al., 1999) – *Bam*HI/T7, *pCMV-SPORT6-Pitx2* (GenBank Accession Number: BC073479) – *Sal*I/T7, *pSK-polaris* (GenBank Accession Number: BJ051594) – *Eco*RI/T7, *pCMV-SPORT6-ROMK* (GenBank Accession Number: CF522101) – *Eco*RI/T7, *pCMV-SPORT6-xSGLT-1K* (Zhou and Vize, 2004) – *Sal*I/T7, *pSK-WT-1* (Carroll and Vize, 1996) – *Bam*HI/T7, *pCS2-Xnr1* (Agius et al., 2000) – *Bam*HI/T7.

Protein analysis, immunohistochemistry and histological analysis

In vitro transcription/translation was performed using the TNT® SP6 Coupled Reticulocyte Lysate System (Promega) and PRO-MIX® L-[^{35}S] *in vitro* cell labeling mix (Amersham). For immunohistochemistry, embryos were fixed in Dent's (4:1 methanol:DMSO), embedded in paraplast, sectioned at 25 μm and stained with the monoclonal anti-acetylated α-tubulin (clone 6-11B-1, Sigma) diluted to 1:1000 or the rabbit anti-NBC1 antibody (Schmitt et al., 1999) diluted to 1:200. For histological staining, embryos were fixed in Bouin's Fixative, dehydrated, embedded in paraplast, sectioned at 7 μm, dewaxed and stained with hematoxylin and eosin.

Results

Developmental expression of Bicaudal-C in the pronephros

Expression of *Bicaudal-C* has previously been reported in the *Xenopus* pronephros (Wessely and De Robertis, 2000). To better characterize this expression domain, whole mount *in situ* hybridizations were performed. *xBic-C* mRNA was first detected in the pronephros in stage 30 *Xenopus* embryos (Fig. 1A). At stage 38, *xBic-C* was observed in the nephrostomes, the pronephric tubules and the duct (Figs. 1B, C). Transverse sections of the stained embryos suggested that *xBic-C* was only expressed in the epithelial structures of the pronephros, but not in the vascular component, the glomus (Figs. 1E, F). This was confirmed by double *in situ* hybridization using *xBic-C* and *Wilms Tumor-1* (*WT-1*), which, at stage 38, is specifically expressed in the glomus (Carroll et al., 1999) and showed complementary non-overlapping staining (Fig. 1G). The same distribution of *xBic-C* mRNA was observed in the mesonephros of adult *Xenopus* using *in situ* hybridization on paraplast sections (data not shown). Taken together these data suggest that *xBic-C* expression is restricted to the renal epithelial cells.

Inhibition of xBic-C results in edema formation

In mouse, mutations in Bicaudal-C lead to polycystic kidney disease in newborn pups (Cogswell et al., 2003). Given that *xBic-C* is expressed in the developing pronephros of the early embryo, we tested whether inhibition of *xBic-C* mRNA

translation in the amphibian pronephros by antisense morpholino oligomers resulted in a PKD-like phenotype. Since *Xenopus laevis* is allotetraploid, two pseudoalleles of *xBic-C* exist. All the original isolates of xBic-C corresponded to one allele (Wessely and De Robertis, 2000) and the sequence of the second allele was identified in the public EST databases (UniGene Cluster Xl.49139). The nucleotide sequences of both alleles around the translational start site were too divergent to be targeted by one antisense morpholino oligomer; therefore, two oligomers (*xBic-C-MO1*, *xBic-C-MO2*) were designed (Fig. 2A). As shown in Fig. 2B, *in vitro* transcription/translation of the approximately 105 kDa xBic-C protein was efficiently inhibited by *xBic-C-MO1*. This block of translation was specific since *xBic-C-MO1* did not inhibit a construct of *xBic-C* mutated in the *xBic-C-MO1* recognition site (*xBic-C**). When either *xBic-C-MO1*, *xBic-C-MO2*, or a mixture of the two antisense morpholino oligomers (*xBic-C-MO1+2*) was injected into 2-cell *Xenopus* embryos, early development proceeded undisturbed, but the embryos started to develop edema at stage 42 (Figs. 2C, D and data not shown). To investigate whether this phenotype was specific for the *xBic-C* antisense morpholino oligomers, we assessed the frequency of edema formation at stage 43 in uninjected embryos and embryos injected with a standard control morpholino oligomer, a scrambled version of *xBic-C-MO2*, *xBic-C-MO1* alone, *xBic-C-MO2* alone and *xBic-C-MO1+2* (Fig. 2E and data not shown). Uninjected embryos or embryos injected with the standard control morpholino oligomer or *BicC-MO2-scrambled* showed negligible edema formation. *xBic-C-MO1* and *xBic-C-MO2*-injected embryos developed edemas in 25% and 63% of the cases, respectively, and the combination of both morpholino oligomers resulted in about 95% edema formation. This effect of the mixture of the two morpholino oligomers was more than additive since microinjection of double amounts of *xBic-C-MO1* or *xBic-C-MO2* alone did not result in such a high incidence of edema formation (Fig. 2E). Based on these results we used the mixture of the two antisense morpholino oligomers (*xBic-C-MO1+2*) in the remainder of this study. We also performed rescue experiments that are described in a later section of the manuscript.

It has been reported that defects in the osmoregulatory function of the pronephros lead to increased water retention and edema formation in amphibian embryos (Howland, 1916). To further investigate whether the phenotype of *xBic-C-MO1+2*-injected embryos is caused by a defect in pronephros function or pronephros formation, histological sections were performed at

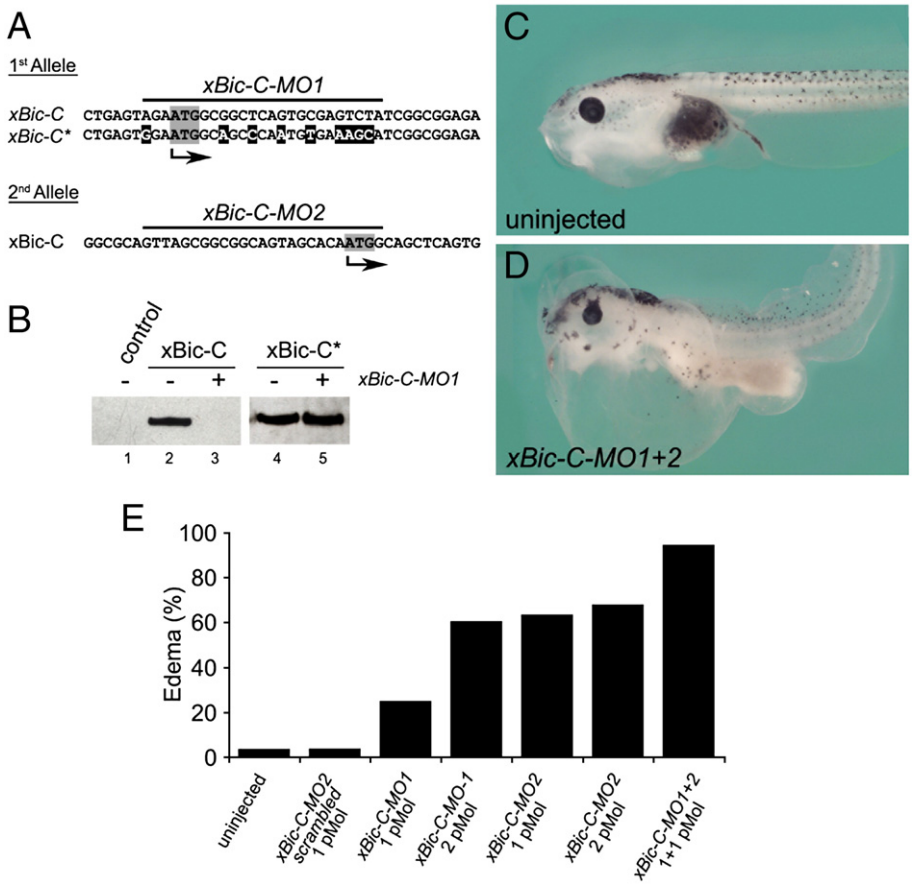

Fig. 2. Inhibition of xBic-C leads to edema formation. (A) Sequence of the two pseudoalleles of *Xenopus Bicaudal-C*. The positions of the two antisense morpholino oligomers are indicated. (B) *In vitro* transcription/translation of xBic-C in the presence or absence of *xBic-C-MO1*. Lane 1, pCSII; lane 2 and 3, *xBic-C-HA*-pCSII; lane 4 and 5, *xBic-C**-*HA*-pCSII. (C, D) Morphology of uninjected and *xBic-C-MO1+2*-injected embryo displaying large edema. (E) Quantification of edema formation at stage 43 of uninjected control embryos and *Xenopus* embryos injected radially at the 2–4 cell stage with *xBic-C-MO2-scrambled* (1 pM), *xBic-C-MO1* (1 pM and 2 pM), *xBic-C-MO2* (1 pM and 2 pM), and *xBic-C-MO1+2* (1 pM each morpholino oligomer).

two different developmental stages. At stage 45, injected embryos displayed an enlarged body cavity, malformations of the endoderm and dilated pronephric tubules (Figs. 3A, B). However, when embryos were analyzed earlier at stage 38, only dilated pronephric tubules were observed (Figs. 3C, D). This suggested that edema formation and the endodermal malformations were secondary to a defect in the developing pronephros.

The physical integrity of the pronephros was confirmed by whole mount *in situ* hybridization using the β1 subunit of the sodium potassium ATPase (*β1-Na/K ATPase*), which is expressed in the pronephric tubules and duct (Eid and Brandli, 2001). Both uninjected control and *xBicC-MO1+2*-injected embryos showed a similar expression pattern (Figs. 3E, F). The pronephric duct is derived from the pronephric rudiment and the rectal diverticulum, which meet and fuse around stage 38 forming a functional pronephros (Schultheiss et al., 2003). One possible explanation for the *xBic-C* morpholino oligomer phenotype was that urine could not be excreted due to defective pronephros development. To address this hypothesis we injected fluorescence labeled 500 kDa Dextran into the heart of the *xBic-C-MO1+2*-injected embryos at stage 42 and followed its filtration path using fluorescence microscopy. As shown in Fig. 3G, fluorescence labeled Dextran was readily excreted by the way of the cloaca. This suggested that a physical barrier impairing fluid flow was not the cause of the dilated tubules in *xBic-C-MO1+2*-injected embryos. Because of the differences in tubule diameters in uninjected and injected embryos (Figs. 3A–D), it was impossible to accurately measure the speed of the fluid flow. Together these data suggested that, in *Xenopus*, Bicaudal-C was not required to establish the tubular structure of the pronephros, but rather played a later role during pronephros development.

Bicaudal-C regulates differentiation of the late distal tubule

It has recently been shown that the pronephros and the individual nephrons in the metanephric kidney share an evolutionarily conserved proximal–distal organization (Zhou and Vize, 2004). To address how inhibition of xBic-C translation affects the functionality of the pronephros we decided to analyze the expression of structural proteins along the proximal–distal axis. Whole mount *in situ* hybridizations were performed on uninjected and *xBic-C-MO1+2*-injected *Xenopus* embryos at stage 38 using a panel of segment-specific marker genes (Fig. 4I). Expression of *Nephrin*, a component of the podocyte slit diaphragm in the glomus (Gerth et al., 2005), *xSGLT-1K*, a sodium glucose transporter present in the proximal tubule, and *NKCC2*, a sodium potassium co-transporter in the early distal tubule (Zhou and Vize, 2004), were not changed (Figs. 4A–C′). The sodium bicarbonate transporter *xNBC1* and *carbonic anhydrase II* (*CAII*) are expressed in the early proximal and the late distal element of the *Xenopus* pronephros regulating acid–base balance (Zhou and Vize, 2004, 2005). In line with the observation that loss-of-xBic-C did not change *SGLT-1K* expression, the expression of *xNBC1* mRNA was unchanged in the proximal tubule as well (Figs. 4D, D′). However, neither *xNBC1* nor *CAII* transcripts could be detected in the late distal element of *xBic-C-MO1+2*-injected embryos (Figs. 4D–E′). *ClC-K* is a kidney specific chloride channel expressed in the early and late distal tubule as well as in the pronephric duct (Vize, 2003). In *xBic-C-MO1+2*-injected embryos *ClC-K* mRNA expression was decreased in the area corresponding to the late distal element at stage 38 (Figs. 4F, F′) and its entire expression in the pronephros was greatly reduced by stage 40 (data not shown). The thiazide sensitive sodium chloride co-

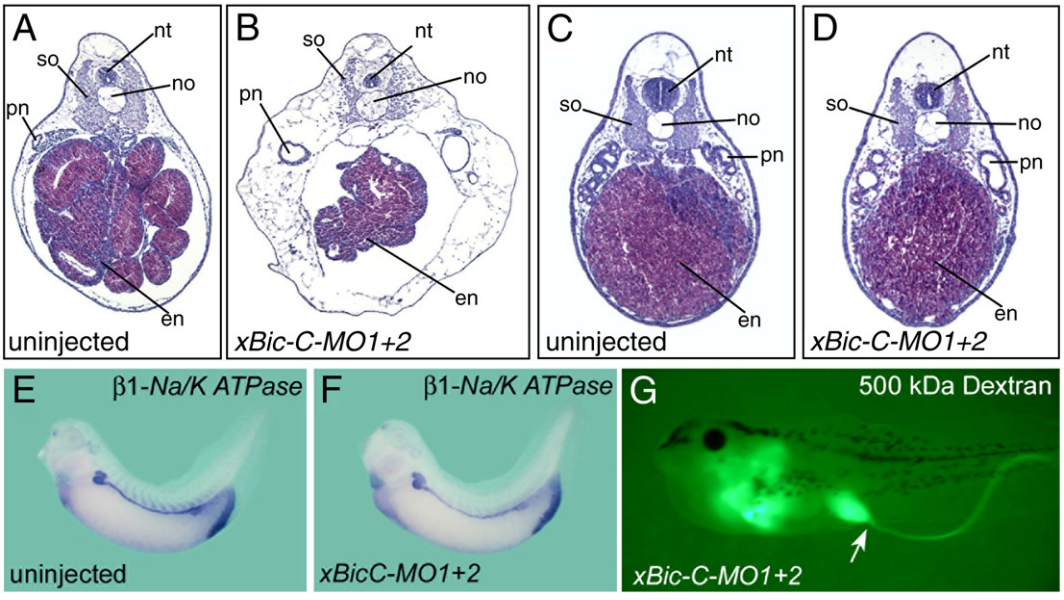

Fig. 3. Bicaudal-C is not required for pronephros formation. (A–D) Histological analysis of transverse sections from uninjected and *xBic-C-MO1+2*-injected embryos at stage 45 (A, B) and stage 38 (C, D). Note the edema and the enlarged pronephric tubules in embryos lacking xBic-C. (E, F) Whole mount *in situ* hybridization of *β1-Na/K ATPase* of uninjected and *xBic-C-MO1+2*-injected embryos. (G) Fluorescence-labeled Dextran injected into the heart of *xBic-C-MO1+2*-injected *Xenopus* embryos is excreted via the pronephros. Arrow indicates the cloaca. en, endoderm; no, notochord; nt, neural tube; pn, pronephros; so, somite.

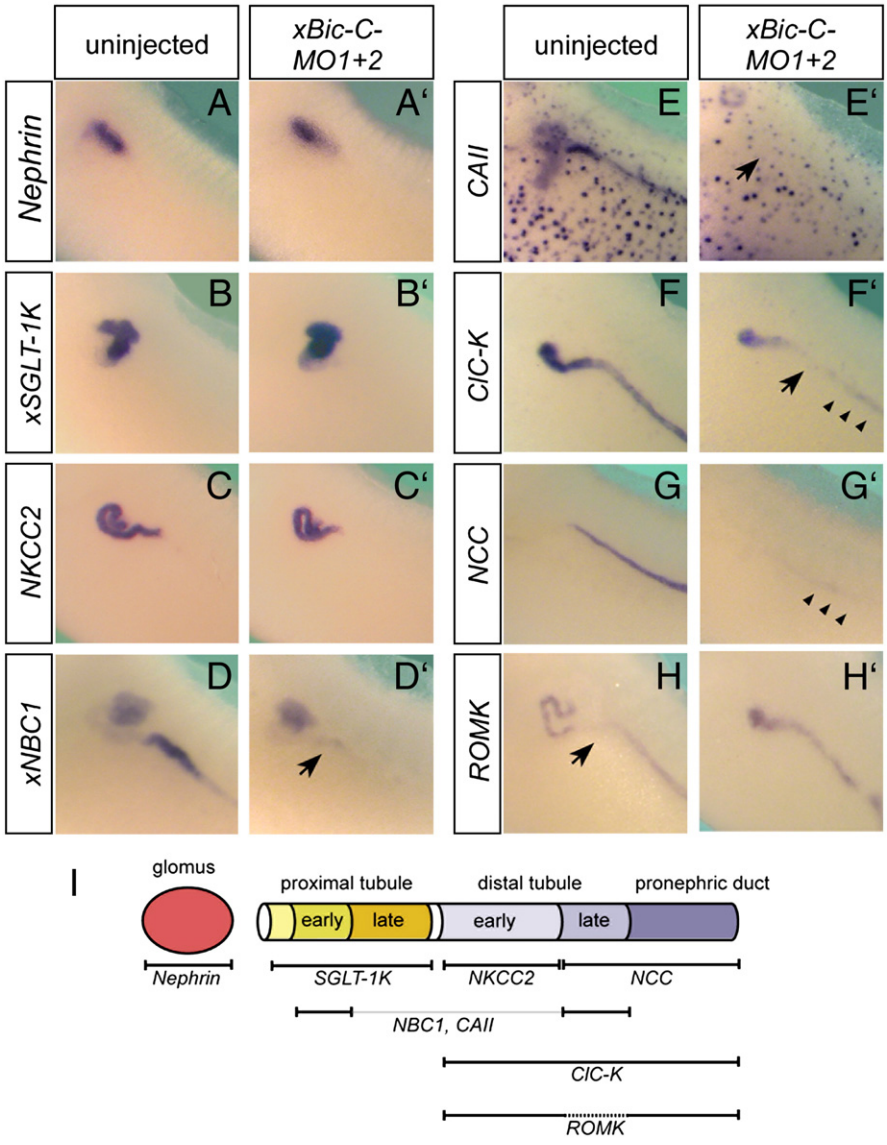

Fig. 4. Expression analysis of pronephric markers. (A–H′) Whole mount *in situ* hybridization analysis of uninjected control and *xBic-C-MO1+2*-injected embryos at stage 38. (A, A′) *Nephrin*; (B, B′) *xSGLT-1K*; (C, C′) *NKCC2*; (D, D′) *xNBC1*; (E, E′) *CAII*; (F, F′) *ClC-K*; (G, G′) *NCC*; (H, H′) *ROMK*. (I) Schematic diagram of the pronephric marker genes used. Arrows point to the late distal pronephric tubule, arrowheads indicate the pronephric duct.

transporter NCC marks the distal convoluted tubule in mammals (Loffing and Kaissling, 2003). We identified an EST encoding *Xenopus* NCC (GenBank Accession # BJ076552). Expression analysis using single and double whole mount *in situ* hybridization of *NCC* and *NKCC2* showed that, in *Xenopus*, *NCC* was expressed in the late distal tubule and the pronephric duct (Fig. 4G and data not shown). Similar to *ClC-K*, *NCC* was greatly reduced in *xBic-C-MO1+2*-injected embryos at stage 38 (Fig. 4G′) and completely absent later (data not shown). Thus, this marker gene analysis demonstrated a defect in the differentiation of the late distal tubule and the pronephric duct. A further marker studied was the *Xenopus* homologue of the rat outer medullary K^+ channel (*ROMK*) (GenBank Accession #CF522101), which in rat is expressed in the thick ascending limb of the Loop of Henle and the principal cells of the cortical collecting ducts (Boim et al., 1995). In *Xenopus*, *ROMK* is strongly expressed in the early distal element and the pronephric duct, but only weakly in the late distal element (Fig. 4H). Upon microinjection of *xBic-C-MO1+2*, *ROMK* was still expressed in the pronephros, but the gap corresponding to the decreased expression in the late distal element was absent. Instead, *ROMK* expression extended uniformly from the early distal element to the pronephric duct (Figs. 4H, H′). To address, whether Bicaudal-C is involved in the induction or maintenance of these genes, the expression of the same marker genes was assessed at earlier stages of pronephric development. Interestingly, markers of the late distal tubule, *xNBC1* and *CAII* were not detected in *xBic-C-MO1+2*-injected embryos at any stage studied (data not shown). Conversely, the molecular markers of the pronephric duct (i.e. *ClC-K* and *NCC*) were expressed at stage 34/35, but were lost subsequently. Taken together, this molecular analysis suggested that Bicaudal-C is required for the expression of terminal differentiation genes in the late distal tubule and parts of the pronephric duct.

Next, we wanted to identify how this defect in gene expression arose. To this end, we analyzed the expression of the transcription factors *GATA-3*, *HNF1β*, *Lim-1*, *Pax-2*, *Pax-8* and *WT-1* in early pronephric development (Figs. 5A–F′). Even though minor differences in gene expression could be detected, only *Lim-1* was significantly changed in the *xBic-C-MO1+2*-injected embryos. In uninjected embryos, as reported earlier (Carroll et al., 1999), *Lim-1* is expressed strongly in the nephrostomes and the pronephric duct and weakly in the tubules at stage 35. In addition, we also detected a yet unreported expression of *Lim-1* in the region corresponding to the late distal tubule (Fig. 5C). It was this expression domain that was specifically lost in the *xBic-C-MO1+2*-injected embryos (Fig. 5C′).

Finally, we wanted to examine whether the observed phenotype was specific for Bicaudal-C. Rescue experiments by co-injection of the mutated *xBic-C** together with *xBic-C-MO1* are very difficult since injection of *xBic-C** mRNA results in ectopic endoderm formation, improper gastrulation movements and embryos do not survive very well (Wessely and De Robertis, 2000). To circumvent this, we decided for the following strategy: *Xenopus* embryos were injected at the 2-cell stage radially with *xBic-C-MO1+2*. At the 4-cell stage, a subset of these embryos were then injected with *xBic-C** mRNA into a single blastomere. Embryos were grown until stage 39 and processed for whole mount *in situ* hybridizations. *NBC1* mRNA was used as the readout for xBic-C activity. As shown above, *NBC1* expression in the late distal tubule was lost upon injection of *xBic-C-MO1+2* (Fig. 4D′). However, *xBic-C** mRNA could recover this *NBC1* expression domain on the injected side (Figs. 5G, H). It was shown in a previous study

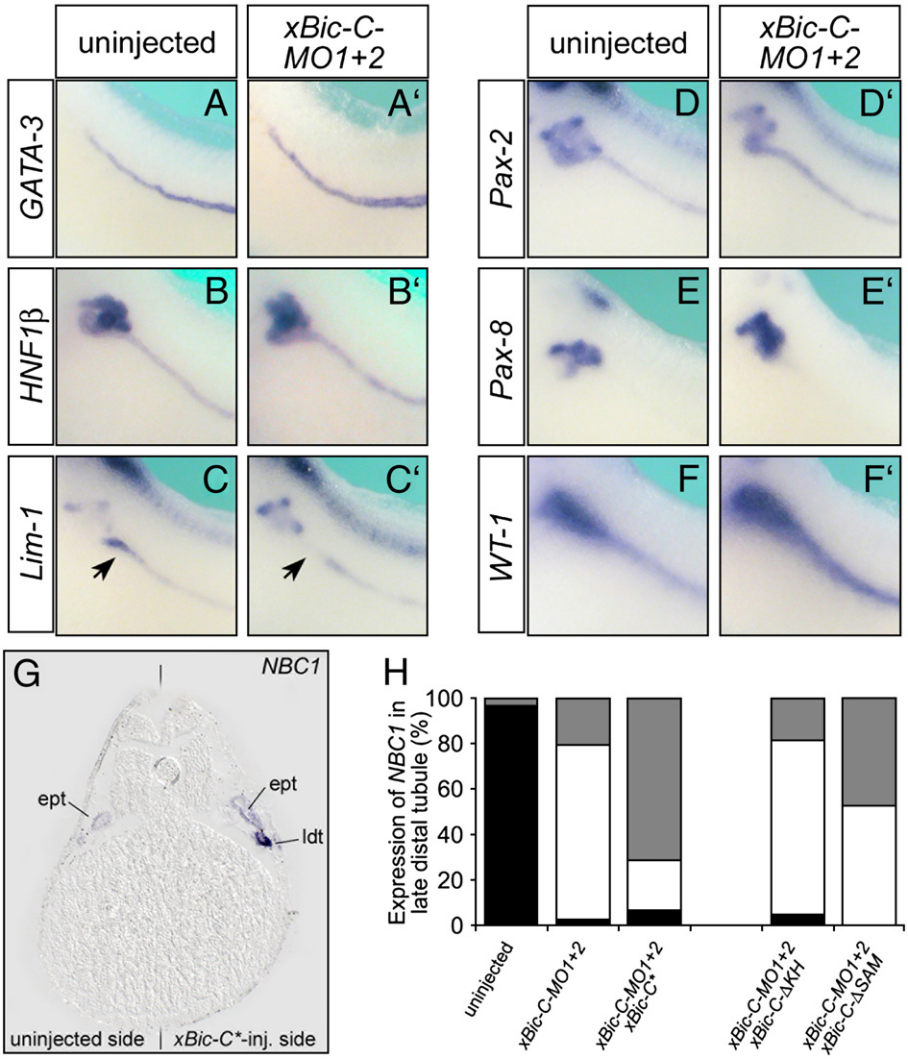

Fig. 5. Expression analysis of transcription factors. (A–F′) Whole mount *in situ* hybridization analysis of uninjected control and *xBic-C-MO1+2*-injected embryos at stage 35. (A, A′) *GATA-3*; (B, B′) *HNF1β*; (C, C′) *Lim-1*; (D, D′) *Pax-2*; (E, E′) *Pax-8*; (F, F′) *WT-1*. Note that the expression of *Lim-1* in the late distal tubule is lost upon microinjection of *xBic-C-MO1+2* (indicated by arrowhead in C, C′). (G, H) Rescue of *NBC1* expression in the late distal tubule in *xBic-C-MO1+2*-injected embryos with a single injection (2 ng) of *xBic-C**, *xBic-C-ΔKH* and *xBic-C-ΔSAM* mRNA. (G) Transverse section showing expression of *NBC1* in the early proximal tubule (ept) and the late distal tubule (ldt). Note that the expression of *NBC1* in the late distal tubule could only be detected on the side injected with *xBic-C** mRNA. (H) Quantification of the expression of *NBC1* in the late distal tubule; black—bilateral expression; white—no expression; gray—unilateral expression rescued by co-injected mRNA. Each of the rescue experiments was performed at least three independent times and the graph depicts the cumulative numbers of all experiments.

(Wessely and De Robertis, 2000) that the RNA-binding domain of Bicaudal-C was required for its activity. In order to test whether the same is true for its function in the pronephros, we performed a rescue experiment using constructs lacking the RNA-binding domain (*xBic-C-ΔKH*) or the protein–protein interaction domain (*xBic-C-ΔSAM*). As shown in Fig. 5H, *xBic-C-ΔSAM* mRNA, but not *xBic-C-ΔKH* mRNA could rescue *NBC1* expression in the late distal tubule. Thus, as during early embryonic development, the RNA-binding domain is crucial for Bicaudal-C activity in the pronephros. Taken together, these data showed that Bicaudal-C is required for the differentiation of the late distal tubule at the transcriptional and structural levels.

Bicaudal-C and cilia formation

Mutations in *Bicaudal-C* in mouse result in PKD (Cogswell et al., 2003). One emerging theme is that PKD is caused by structural or functional defects in primary cilia present on the renal epithelial cells of the metanephric kidney (Nauli et al., 2003). Therefore, we decided to address whether the loss-of-xBic-C phenotype in *Xenopus* embryos is connected to cilia function. Genes such as *FoxJI*, *Axonemal Dynein Heavy Chain 9* (*ADHC9*) and *Tg737*/*polaris* are involved in the formation of motile cilia (Yoder et al., 2002b; Gomperts et al., 2004; Kramer-Zucker et al., 2005). *In situ* hybridizations of these genes at stage 36 showed staining in the ciliated cells of the epidermis and the nephrostomes, but no mRNA expression could be detected in the pronephric tubules and duct (Figs. 6A–C). On the other hand, *xBic-C* was expressed in the nephrostomes, but could not be detected in the ciliated cells of the epidermis (Figs. 1A–C). Moreover, microinjection of *xBic-C-MO1+2* did not affect the expression of any of these genes (Fig. 6D and data not shown). These data suggested that xBic-C did not regulate the transcription of genes involved in the formation of motile cilia, but showed some overlap with their expression.

To directly test whether xBic-C is involved with cilia formation, paraplast sections of uninjected and *xBic-C-MO1+2*-injected embryos were stained at stage 40 with a cilia marker, anti-acetylated α-tubulin antibody (Essner et al., 2002). Uninjected *Xenopus* embryos showed high expression of acetylated tubulin in the ciliated cells of the epidermis and in the cells surrounding the nephrostomes (Figs. 6E, F). In the remainder of the pronephros the majority of renal epithelial cells express about one cilium per cell (Fig. 6G and data not shown). When comparing the uninjected and the *xBic-C-MO1+2*-injected embryos, no obvious differences in the number of the cilia were detected in any of these locations (Figs. 6E–G′).

It has been shown that loss-of-Polaris results in stunted cilia in mouse (Yoder et al., 2002b) and pronephric cyst formation as a consequence of impaired ciliogenesis in zebrafish (Kramer-Zucker et al., 2005). Therefore, as a control to the Bic-C loss of function, cilia formation in *xPol-MO*-injected embryos was studied. Similar to zebrafish, *Xenopus* embryos lacking Polaris protein developed edema by stage 38 (Supplemental Fig. S1). Furthermore, *xPol-MO*-injected embryos displayed reduced acetylated α-tubulin staining in the ciliated cells of the epidermis (Figs. 6H, H′) and the nephrostomes (Figs. 6I, I′). In agreement with the expression data, which did not detect *polaris* mRNA in the pronephric tubules and duct (Fig. 6C), no differences in acetylated α-tubulin staining were seen in these cells (Figs. 6J, J′ and data not shown).

To further strengthen this argument we directly compared the length of individual cilia in the *Xenopus* pronephros. Preliminary experiments in uninjected control embryos showed that the length of the cilia was not homogenous throughout the pronephric tubules and duct (data not shown). Thus, double immunostaining with antibodies for NBC1 (Schmitt et al., 1999) and acetylated α-tubulin was used to detect cilia in the early proximal tubules. As shown in Figs. 6K, K′, no significant differences could be observed in uninjected control and *xBic-C-MO1+2*-injected embryos. Together, these data support our observation that Bicaudal-C, in contrast to Polaris, is not involved in cilia formation.

Discussion

Bicaudal-C and PKD

Genes involved in polycystic kidney disease (PKD) have been successfully studied in a variety of model systems (Drummond et al., 1998; Guay-Woodford, 2003; Sun et al., 2004). Here we report – for the first time – that the *Xenopus* pronephros can serve as an equally useful system to study PKD pathogenesis as well as mechanisms of terminal epithelial differentiation. Several lines of evidence demonstrate that elimination of Bicaudal-C protein using antisense morpholino oligomers may have resulted in a PKD-like phenotype in *Xenopus*: (i) nearly all *xBic-C-MO1+2*-injected embryos developed edema (Figs. 2D, E). Since frogs constantly take up water through the skin and in the course of feeding, large volumes of urine have to be excreted to maintain osmotic balance. The pronephros is essential for the control of water balance. The lack of a functional pronephros leads to the accumulation of body fluids in the coelomic cavity resulting in edema formation (Howland, 1916). However, edema formation cannot be used as the only criterion for a PKD-like phenotype. For instance, *Xenopus* embryos microinjected with an antisense morpholino oligomer against *Wilms′ Tumor Gene-1* (*WT-1*) developed edema not because of defects in the pronephric duct or tubules, but because WT-1 is required for the proper development of the blood-filtering glomus (unpublished observations). (ii) *Xenopus* embryos lacking Bicaudal-C displayed an increased tubule diameter throughout the pronephric tubules and duct (Figs. 3D and 6G′). This phenotype is reminiscent of all forms of human PKD, which is caused by uncontrolled expansion of renal tubules (Sutters and Germino, 2003; Wilson, 2004). (iii) No changes in the early phases of pronephros formation could be detected in *xBic-C-MO1+2*-injected embryos. The early expression patterns of transcription factors regulating pronephros development such as *GATA-3*, *HNF1β*, *pax-2*, *pax-8* and *WT-1* were unaltered (Figs. 5A–F′). Furthermore, the pronephric rudiment and the rectal diverticulum fused in a timely manner and formed a contiguous pronephric system (Fig. 3G). Similarly, in PKD, individual nephrons initially develop

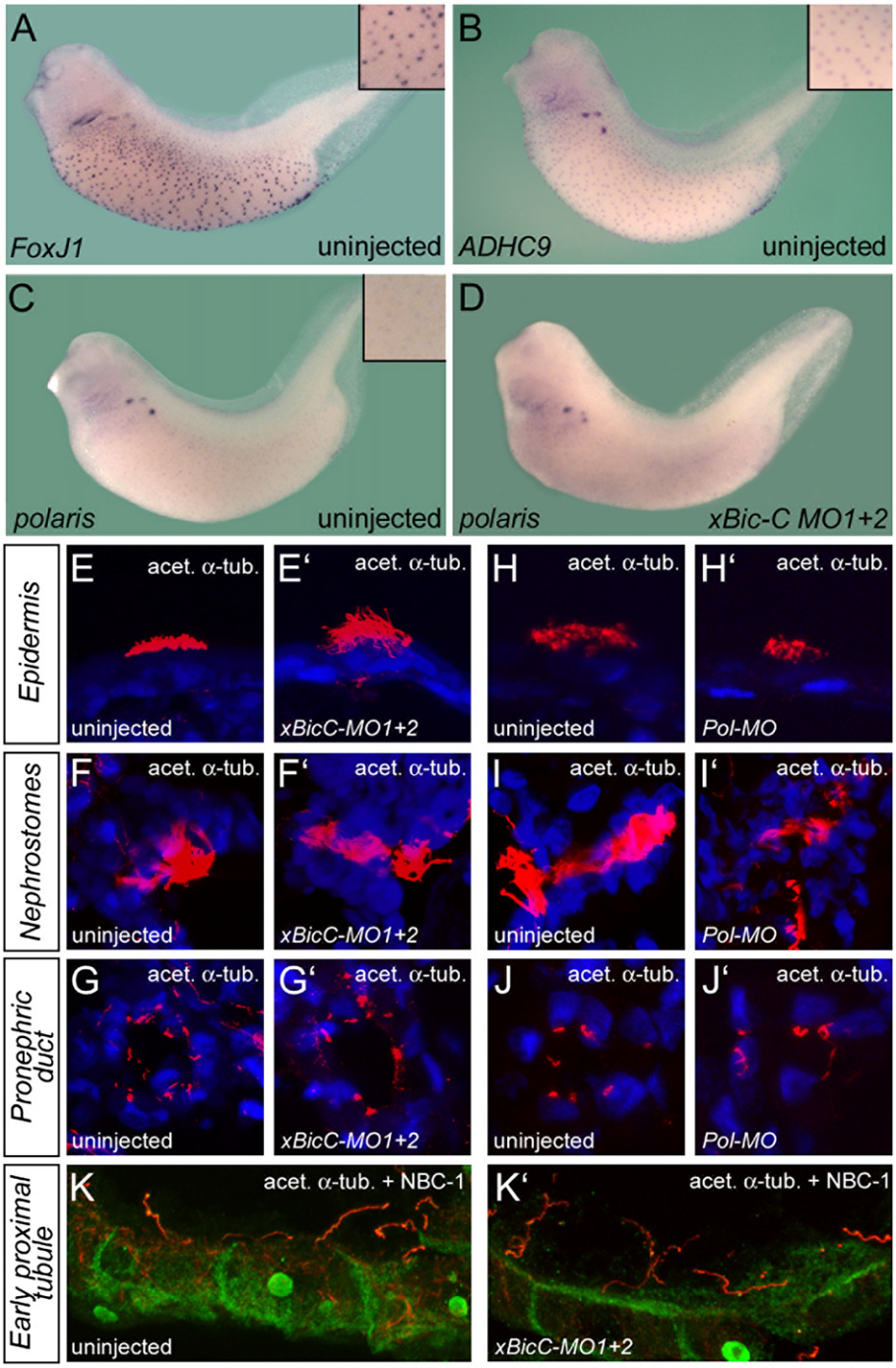

Fig. 6. Bicaudal-C and cilia formation. (A–D) Whole mount *in situ* hybridization of uninjected (A–C) or *xBic-C-MO1+2*-injected *Xenopus* embryos (D) at stage 36 using (A) *FoxJ1*, (B) *Axonemal Dynein Heavy Chain 9* (*ADHC9*) and (C, D) *polaris*. (E–J′) Immunocytochemistry using anti-acetylated α-tubulin antibody (red) on uninjected control, *xBic-C-MO1+2* and *xPol-MO*-injected embryos at stage 42. (E, E′, H, H′) Ciliated cells of the epidermis; (F, F′, I, I′) cilia of the nephrostomes; (G, G′, J, J′) individual primary cilia present on the cells of the pronephric duct. (K, K′) Immunocytochemistry using anti-acetylated α-tubulin (red) and anti-NBC1 (green) antibodies on uninjected control and *xBic-C-MO1+2*-injected embryos at stage 42. Images were obtained by confocal microscopy; nuclei were counterstained with DAPI (blue).

normally and only secondarily undergo tubular expansion (Wilson, 2004).

The molecular mechanisms leading to polycystic kidney disease are still poorly understood. Research currently focuses on the three genes mutated in human polycystic kidney disease, *PKD1*, *PKD2* and *PKHD1* (Sutters and Germino, 2003; Wilson, 2004). However, many additional genes have been shown to result in PKD in mouse, rat and zebrafish and these studies have contributed significantly to a better understanding of the disease (Guay-Woodford, 2003). Among them, the RNA-binding molecule Bicaudal-C is the least understood and has not yet been incorporated into the emerging picture of PKD. We

addressed the molecular mechanism underlying the PKD-like phenotype in *Xenopus* embryos that lack Bicaudal-C. Interestingly, preliminary data suggest that loss of Bicaudal-C as other PKD genes also disrupts the patterning of the left–right body axis (data not shown). One intriguing hypothesis was that Bicaudal-C is involved in the formation/assembly of cilia since those have been shown to be involved in PKD and left–right patterning. However, inhibition of Bicaudal-C in *Xenopus* did not change the presence or appearance of the cilia present on the epithelial cells in the pronephros (Figs. 6E–G′, K, K′). Similarly, electron microscopy of principal cells derived from the collecting duct of *bpk* mice (carrying a hypomorphic allele of *Bicaudal-C*) exhibits normal cilia (Veizis et al., 2004). Thus, a more likely hypothesis is that the function of Bicaudal-C is required downstream of cilia formation in regulating cilia function. This scenario is difficult to address. Even though ciliogenesis has been studied extensively over the past couple of years, only few reliable read-out systems for cilia function, such as the imaging of calcium waves caused by cilia bending, exist.

Cilia and the Xenopus pronephros

The *Xenopus* pronephros is a simple, non-integrated nephron (Fig. 1D). The glomus releases the blood filtrate into the coelomic cavity, which is then transported via the three nephrostomes into the pronephric tubules. The cells surrounding the nephrostomes are multiciliated with a classical 9+2 microtubular arrangement, while the renal epithelial cells in the pronephric tubule and duct contain one primary cilia (Mobjerg et al., 2000; Vize et al., 2003). Interfering with the formation of the cilia in the nephrostomes by inhibiting Polaris function resulted in edema formation (Supplemental Fig. S1). This was probably caused by the inability of the nephrostomes to move the filtrate from the nephrocoelom into the pronephric tubules. But in contrast to *Bic-C-MO-1+2*, injection of *Pol-MO* did not measurably affect the diameter of the pronephric tubules and duct. The anatomy of the amphibian pronephros is different from the one of zebrafish and other teleosts, which has a pronephros that more closely resembles a mesonephric nephron. In zebrafish, the tubules and the glomus are closely associated; the filtrate is directly taken up by the tubules and the function of the nephrostomes is not required (Drummond et al., 1998). Multi- and monociliated cells are found throughout the pronephros to move the filtrate along, and cilia-associated genes are expressed in the entire pronephros (Bisgrove et al., 2005; Kramer-Zucker et al., 2005; Liu et al., 2007). As a consequence of these anatomical differences, inhibition of ciliogenesis in zebrafish results in the formation of cysts in the pronephros itself and not – like in *Xenopus* – in edema (Kramer-Zucker et al., 2005).

Interestingly, genes such as *FoxJ1*, *polaris* or *ADHC9*, all of which have been shown to be involved in different aspects of ciliogenesis (Yoder et al., 2002b; Gomperts et al., 2004; Kramer-Zucker et al., 2005), displayed an almost identical expression pattern in *Xenopus*. All of them were co-expressed in the nephrostomes of the pronephros, the ciliated cells of the epidermis, the developing pancreas and the late dorsal blastopore lip (Figs. 6A–C and data not shown). Thus, *FoxJ1*, *polaris* and *ADHC9* could be regarded as members of a cilia synexpression group (Niehrs and Pollet, 1999). This group probably contains many more proteins. A genomics approach in *Chlamydomonas* has identified more than 250 proteins that may be involved in ciliogenesis (Li et al., 2004). Similarly, genetic screens in zebrafish and *C. elegans* have identified several of these genes (Drummond et al., 1998; Sun et al., 2004; Barr, 2005). Cilia play an instrumental role not only in the kidney, but also in the pancreas (Cano et al., 2004), in the establishment of the left–right body axis (McGrath et al., 2003) and in limb development (Haycraft et al., 2005; Huangfu and Anderson, 2005).

It is noteworthy that the expression of *Bicaudal-C* only shows a partial overlap to this group of genes involved in ciliogenesis. *Bicaudal-C* is expressed in the epithelial cells of the pronephros (including nephrostomes) and the late dorsal blastopore lip, but not in the ciliated cells of the skin (Figs. 1B, C, 6A–C, Wessely and De Robertis, 2000 and data not shown). In addition, no transcriptional cross-regulation between Bicaudal-C and cilia-associated genes could be detected. *xBic-C-MO1+2*-injected embryos did not display changes in the expression of *FoxJ1*, *polaris* and *ADHC9*, nor did *xPol-MO* injections alter *xBic-C* mRNA expression (Figs. 6C, D and data not shown). However, the loss of Bicaudal-C resulted in phenotypes reminiscent of defects in cilia function, i.e. PKD and defects in left–right patterning (this manuscript and unpublished observations) suggesting a yet-to-be-identified connection between Bicaudal-C and cilia.

Bicaudal-C and pronephros development

The functionality of the kidney relies entirely on the proper organization and differentiation of the individual segments within the nephron. However, very little information is available about the factors determining proximal–distal identities (Carroll and McMahon, 2003). Even in mouse, only a small number of genes such as *Brn-1* and *FoxI1* have been shown to have segment-specific functions (Nakai et al., 2003; Blomqvist et al., 2004). Furthermore, Delta/Notch pathway is the only signaling system, which regulates proximal–distal nephron patterning (Cheng et al., 2003, 2007; Wang et al., 2003), but has also been shown to be necessary for the differentiation of a specific cell type within the zebrafish pronephros, the multiciliated cells (Liu et al., 2007).

In contrast to these genes, which show highly restricted segment-specific expression, *Bicaudal-C* mRNA is not restricted to a particular nephron segment. Instead, it can be detected in all epithelial cells of the pronephros (Fig. 1). Furthermore, histological analysis of the pronephros in *xBic-C-MO1+2*-injected *Xenopus* embryos demonstrated a dilated tubule diameter along the entire length of the pronephros (Figs. 3A–D, Figs. 6G, G′ and data not shown). This suggested that embryos lacking Bic-C had a pronephric-wide defect. We have addressed this scenario by analyzing the expression patterns of an extensive list of marker genes (Figs. 4, 5 and data not shown), but did not detect the expression of any genes altered

throughout the pronephric kidney. Instead, the only genes changed were those specifically expressed in the late distal tubule. Marker genes expressed in the late distal tubule such as *NBC1* and *carbonic anhydrase II* were completely dependent on xBic-C. Furthermore, these changes were not limited to functional proteins, but could be extended to the transcription factor *Lim-1*. We showed that, in addition to the previously reported expression pattern, *Lim-1* was specifically expressed in the late distal tubule and was lost in this region upon injection of *xBic-C-MO1+2* (Figs. 5C, C′). This suggested a scenario in which xBic-C regulates the expression of *Lim-1*, which then in turn is directly required for the terminal differentiation of the late distal tubule. In *Xenopus*, studies using a Lim-1-Engrailed fusion protein have shown that Lim-1 is required for the formation of the pronephric tubules, but not the pronephric duct (Chan et al., 2000). In mouse, Lim-1 has multiple roles during kidney development (Kobayashi et al., 2005). A similar scenario in frog is likely as well. *Lim-1* also exhibits a dynamic expression pattern during pronephros development (Carroll et al., 1999). In the future, it will be very interesting to see how Bicaudal-C regulates *Lim-1* expression. This may shed some light on how a gene expressed throughout the pronephric tubules and duct can have such a segment-specific phenotype, when eliminated.

The molecular mechanism underlying Bicaudal-C activity is still unclear. The rescue experiments of the *xBic-C-MO1+2* phenotype (Fig. 5H) indicate that the RNA-binding activity, but not the SAM domain of Bicaudal-C is required for its function in the pronephros. This correlates well with studies in other organisms. In *C. elegans*, a close relative of Bicaudal-C, GLD-3, binds to the cytoplasmic poly-A-polymerase, GLD-2, and targets specific mRNAs for polyadenylation and increased expression (Wang et al., 2002). Similarly, in *Drosophila*, Bicaudal-C regulates translation of the posterior determinant Oskar (Saffman et al., 1998). Therefore, it is likely that xBic-C regulates localized mRNA translation and it will be very important to identify these targets in future studies. In a first attempt, we have analyzed a panel of transcription factors expressed in the pronephros and have shown that the expression of *Lim-1* in the late distal tubule was lost upon inhibition of xBic-C (Figs. 5C, C′). Another candidate is TGF-β signaling. Earlier studies in *Xenopus* have shown that microinjection of *xBic-C* mRNA results in ectopic endoderm formation by modulating endogenous Nodal/Activin signaling (Wessely and De Robertis, 2000). However, even though in mouse, TGF-β family members are expressed in the kidney and regulate many aspects of kidney organogenesis, they have not yet been shown to be involved in the proximal–distal axis patterning of individual nephrons (Oxburgh et al., 2004).

In summary, this study demonstrates that Bicaudal-C is an important factor in the formation of a functional pronephric kidney. It exemplifies the importance to explore kidney development in different animal systems to understand kidney diseases. While PKD has been intensively studied for many years, its pathobiology at the cellular and molecular level has only recently been the focus of intense investigation. The amphibian pronephros will be a valuable tool in this undertaking. It should help in devising novel treatment strategies against PKD, which are not targeted to alleviate a fully developed disease phenotype, but rather interfere with its onset.

Acknowledgments

U.T. and O.W. would like to thank Dr. Eddy De Robertis for his invaluable guidance during their time at HHMI/UCLA. We also thank Drs. S. El-Dahr, J. Larraín, M. Oelgeschläger, E. Pera and S. Piccolo and all members of the laboratory for critically reviewing the manuscript and helpful discussions, Drs. P. Vize, R. Vignali, A. Brändli and the NIBB/NIG/NBRP *Xenopus laevis* EST project for plasmids and Dr. W. Boron for the NBC1 antibody. We also would like to thank many of our vendors, in particular GeneTools, for their generous support to replenish materials lost due to Hurricane Katrina. L.M.P. was a summer student in the Louisiana Cancer Research Consortium National Cancer Institute Summer Research Internship Program. This work was supported by grants from the Polycystic Kidney Disease Foundation (#103a2r) and NIH/NIDDK (#5R21DK070671-02).

Appendix A. Supplementary data

Supplementary data associated with this article can be found, in the online version, at doi:10.1016/j.ydbio.2007.04.030.

References

Agius, E., Oelgeschläger, M., Wessely, O., Kemp, C., De Robertis, E.M., 2000. Endodermal Nodal-related signals and mesoderm induction in *Xenopus*. Development 127, 1173–1183.

Barr, M.M., 2005. *Caenorhabditis elegans* as a model to study renal development and disease: sexy cilia. J. Am. Soc. Nephrol. 16, 305–312.

Barr, M.M., DeModena, J., Braun, D., Nguyen, C.Q., Hall, D.H., Sternberg, P.W., 2001. The *Caenorhabditis elegans* autosomal dominant polycystic kidney disease gene homologs lov-1 and pkd-2 act in the same pathway. Curr. Biol. 11, 1341–1346.

Bisgrove, B.W., Snarr, B.S., Emrazian, A., Yost, H.J., 2005. Polaris and Polycystin-2 in dorsal forerunner cells and Kupffer's vesicle are required for specification of the zebrafish left–right axis. Dev. Biol. 287, 274–288.

Blomqvist, S.R., Vidarsson, H., Fitzgerald, S., Johansson, B.R., Ollerstam, A., Brown, R., Persson, A.E., Bergstrom, G.G., Enerback, S., 2004. Distal renal tubular acidosis in mice that lack the forkhead transcription factor Foxi1. J. Clin. Invest. 113, 1560–1570.

Boim, M.A., Ho, K., Shuck, M.E., Bienkowski, M.J., Block, J.H., Slightom, J.L., Yang, Y., Brenner, B.M., Hebert, S.C., 1995. ROMK inwardly rectifying ATP-sensitive K+ channel. II. Cloning and distribution of alternative forms. Am. J. Physiol. 268, F1132–F1140.

Cano, D.A., Murcia, N.S., Pazour, G.J., Hebrok, M., 2004. Orpk mouse model of polycystic kidney disease reveals essential role of primary cilia in pancreatic tissue organization. Development 131, 3457–3467.

Carroll, T.J., McMahon, A.P., 2003. Overview: the molecular basis of kidney development. In: Vize, P.D., Woolf, A.S., Bard, J.B.L. (Eds.), The Kidney: From Normal Development to Congenital Disease. Academic Press, Amsterdam, pp. 343–376.

Carroll, T.J., Vize, P.D., 1996. Wilms' tumor suppressor gene is involved in the development of disparate kidney forms: evidence from expression in the *Xenopus* pronephros. Dev. Dyn. 206, 131–138.

Carroll, T.J., Wallingford, J.B., Vize, P.D., 1999. Dynamic patterns of gene expression in the developing pronephros of *Xenopus laevis*. Dev. Genet. 24, 199–207.

Chan, T.C., Takahashi, S., Asashima, M., 2000. A role for Xlim-1 in pronephros development in *Xenopus laevis*. Dev. Biol. 228, 256–269.

Cheng, H.T., Miner, J.H., Lin, M., Tansey, M.G., Roth, K., Kopan, R., 2003. Gamma-secretase activity is dispensable for mesenchyme-to-epithelium transition but required for podocyte and proximal tubule formation in developing mouse kidney. Development 130, 5031–5042.

Cheng, H.T., Kim, M., Valerius, M.T., Surendran, K., Schuster-Gossler, K., Gossler, A., McMahon, A.P., Kopan, R., 2007. Notch2, but not Notch1, is required for proximal fate acquisition in the mammalian nephron. Development 134, 801–811.

Cogswell, C., Price, S.J., Hou, X., Guay-Woodford, L.M., Flaherty, L., Bryda, E.C., 2003. Positional cloning of jcpk/bpk locus of the mouse. Mamm. Genome 14, 242–249.

Drummond, I.A., 2005. Kidney development and disease in the zebrafish. J. Am. Soc. Nephrol. 16, 299–304.

Drummond, I.A., Majumdar, A., Hentschel, H., Elger, M., Solnica-Krezel, L., Schier, A.F., Neuhauss, S.C., Stemple, D.L., Zwartkruis, F., Rangini, Z., Driever, W., Fishman, M.C., 1998. Early development of the zebrafish pronephros and analysis of mutations affecting pronephric function. Development 125, 4655–4667.

Eid, S.R., Brandli, A.W., 2001. *Xenopus* Na,K-ATPase: primary sequence of the beta2 subunit and *in situ* localization of alpha1, beta1, and gamma expression during pronephric kidney development. Differentiation 68, 115–125.

Essner, J.J., Vogan, K.J., Wagner, M.K., Tabin, C.J., Yost, H.J., Brueckner, M., 2002. Conserved function for embryonic nodal cilia. Nature 418, 37–38.

Flaherty, L., Bryda, E.C., Collins, D., Rudofsky, U., Montogomery, J.C., 1995. New mouse model for polycystic kidney disease with both recessive and dominant gene effects. Kidney Int. 47, 552–558.

Gerth, V.E., Zhou, X., Vize, P.D., 2005. Nephrin expression and three-dimensional morphogenesis of the *Xenopus* pronephric glomus. Dev. Dyn. 233, 1131–1139.

Gomperts, B.N., Gong-Cooper, X., Hackett, B.P., 2004. Foxj1 regulates basal body anchoring to the cytoskeleton of ciliated pulmonary epithelial cells. J. Cell Sci. 117, 1329–1337.

Guay-Woodford, L.M., 2003. Murine models of polycystic kidney disease: molecular and therapeutic insights. Am. J. Physiol.: Renal Physiol. 285, F1034–F1049.

Haycraft, C.J., Banizs, B., Aydin-Son, Y., Zhang, Q., Michaud, E.J., Yoder, B.K., 2005. Gli2 and gli3 localize to cilia and require the intraflagellar transport protein polaris for processing and function. PLoS Genet. 1, e53.

Hildebrandt, F., Otto, E., Rensing, C., Nothwang, H.G., Vollmer, M., Adolphs, J., Hanusch, H., Brandis, M., 1997. A novel gene encoding an SH3 domain protein is mutated in nephronophthisis type 1. Nat. Genet. 17, 149–153.

Howland, R.B., 1916. On the effect of removal of the pronephros of the amphibian embryo. Proc. Natl. Acad. Sci. U. S. A. 2, 231–234.

Huangfu, D., Anderson, K.V., 2005. Cilia and Hedgehog responsiveness in the mouse. Proc. Natl. Acad. Sci. U. S. A. 102, 11325–11330.

Hughes, J., Ward, C.J., Peral, B., Aspinwall, R., Clark, K., San Millan, J.L., Gamble, V., Harris, P.C., 1995. The polycystic kidney disease 1 (PKD1) gene encodes a novel protein with multiple cell recognition domains. Nat. Genet. 10, 151–160.

Jones, E.A., 2003. Molecular control of pronephric development: an overview. In: Vize, P.D., Woolf, A.S., Bard, J.B.L. (Eds.), The Kidney: From Normal Development to Congenital Disease. Academic Press, Amsterdam, pp. 93–117.

Jones, E.A., 2005. *Xenopus*: a prince among models for pronephric kidney development. J. Am. Soc. Nephrol. 16, 313–321.

Kobayashi, A., Kwan, K.M., Carroll, T.J., McMahon, A.P., Mendelsohn, C.L., Behringer, R.R., 2005. Distinct and sequential tissue-specific activities of the LIM-class homeobox gene Lim1 for tubular morphogenesis during kidney development. Development 132, 2809–2823.

Kramer-Zucker, A.G., Olale, F., Haycraft, C.J., Yoder, B.K., Schier, A.F., Drummond, I.A., 2005. Cilia-driven fluid flow in the zebrafish pronephros, brain and Kupffer's vesicle is required for normal organogenesis. Development 132, 1907–1921.

Li, J.B., Gerdes, J.M., Haycraft, C.J., Fan, Y., Teslovich, T.M., May-Simera, H., Li, H., Blacque, O.E., Li, L., Leitch, C.C., Lewis, R.A., Green, J.S., Parfrey, P.S., Leroux, M.R., Davidson, W.S., Beales, P.L., Guay-Woodford, L.M., Yoder, B.K., Stormo, G.D., Katsanis, N., Dutcher, S.K., 2004. Comparative genomics identifies a flagellar and basal body proteome that includes the BBS5 human disease gene. Cell 117, 541–552.

Liu, S., Lu, W., Obara, T., Kuida, S., Lehoczky, J., Dewar, K., Drummond, I.A., Beier, D.R., 2002. A defect in a novel Nek-family kinase causes cystic kidney disease in the mouse and in zebrafish. Development 129, 5839–5846.

Liu, Y., Pathak, N., Kramer-Zucker, A., Drummond, I.A., 2007. Notch signaling controls the differentiation of transporting epithelia and multiciliated cells in the zebrafish pronephros. Development 134, 1111–1122.

Loffing, J., Kaissling, B., 2003. Sodium and calcium transport pathways along the mammalian distal nephron: from rabbit to human. Am. J. Physiol.: Renal Physiol. 284, F628–F643.

McGrath, J., Somlo, S., Makova, S., Tian, X., Brueckner, M., 2003. Two populations of node monocilia initiate left–right asymmetry in the mouse. Cell 114, 61–73.

Mobjerg, N., Larsen, E.H., Jespersen, A., 2000. Morphology of the kidney in larvae of *Bufo viridis* (Amphibia, Anura, Bufonidae). J. Morphol. 245, 177–195.

Mochizuki, T., Wu, G., Hayashi, T., Xenophontos, S.L., Veldhuisen, B., Saris, J.J., Reynolds, D.M., Cai, Y., Gabow, P.A., Pierides, A., Kimberling, W.J., Breuning, M.H., Deltas, C.C., Peters, D.J., Somlo, S., 1996. PKD2, a gene for polycystic kidney disease that encodes an integral membrane protein. Science 272, 1339–1342.

Mohler, J., Wieschaus, E.F., 1986. Dominant maternal-effect mutations of *Drosophila melanogaster* causing the production of double-abdomen embryos. Genetics 112, 803–822.

Nakai, S., Sugitani, Y., Sato, H., Ito, S., Miura, Y., Ogawa, M., Nishi, M., Jishage, K., Minowa, O., Noda, T., 2003. Crucial roles of Brn1 in distal tubule formation and function in mouse kidney. Development 130, 4751–4759.

Nauli, S.M., Alenghat, F.J., Luo, Y., Williams, E., Vassilev, P., Li, X., Elia, A.E., Lu, W., Brown, E.M., Quinn, S.J., Ingber, D.E., Zhou, J., 2003. Polycystins 1 and 2 mediate mechanosensation in the primary cilium of kidney cells. Nat. Genet. 33, 129–137.

Nauta, J., Ozawa, Y., Sweeney Jr., W.E., Rutledge, J.C., Avner, E.D., 1993. Renal and biliary abnormalities in a new murine model of autosomal recessive polycystic kidney disease. Pediatr. Nephrol. 7, 163–172.

Niehrs, C., Pollet, N., 1999. Synexpression groups in eukaryotes. Nature 402, 483–487.

Nieuwkoop, P.D., Faber, J., 1994. Normal Table of *Xenopus laevis*. Garland Publishing, Inc., New York.

Obara, T., Mangos, S., Liu, Y., Zhao, J., Wiessner, S., Kramer-Zucker, A.G., Olale, F., Schier, A.F., Drummond, I.A., 2006. Polycystin-2 immunolocalization and function in zebrafish. J. Am. Soc. Nephrol. 17, 2706–2718.

Otto, E.A., Schermer, B., Obara, T., O'Toole, J.F., Hiller, K.S., Mueller, A.M., Ruf, R.G., Hoefele, J., Beekmann, F., Landau, D., Foreman, J.W., Goodship, J.A., Strachan, T., Kispert, A., Wolf, M.T., Gagnadoux, M.F., Nivet, H., Antignac, C., Walz, G., Drummond, I.A., Benzing, T., Hildebrandt, F., 2003. Mutations in INVS encoding inversin cause nephronophthisis type 2, linking renal cystic disease to the function of primary cilia and left–right axis determination. Nat. Genet. 34, 413–420.

Oxburgh, L., Chu, G.C., Michael, S.K., Robertson, E.J., 2004. TGFbeta superfamily signals are required for morphogenesis of the kidney mesenchyme progenitor population. Development 131, 4593–4605.

Pfaller, W., Klima, J., 1976. A critical reevaluation of the structure of the rat uriniferous tubule as revealed by scanning electron microscopy. Cell. Tissue Res. 166, 91–100.

Saffman, E.E., Styhler, S., Rother, K., Li, W., Richard, S., Lasko, P., 1998. Premature translation of *oskar* in oocytes lacking the RNA-binding protein Bicaudal-C. Mol. Cell. Biol. 18, 4855–4862.

Saxén, L., 1987. Organogenesis of the Kidney. Cambridge Univ. Press, Cambridge, UK.

Schmitt, B.M., Biemesderfer, D., Romero, M.F., Boulpaep, E.L., Boron, W.F., 1999. Immunolocalization of the electrogenic Na+–HCO-3 cotransporter in mammalian and amphibian kidney. Am. J. Physiol. 276, F27–F38.

Schultheiss, T.M., James, R.G., Listopadova, A., Herzlinger, D., 2003. Formation of the nephric duct. In: Vize, P.D., Woolf, A.S., Bard, J.B.L. (Eds.), The Kidney: From Normal Development to Congenital Disease. Academic Press, Amsterdam, pp. 51–60.

Schweickert, A., Weber, T., Beyer, T., Vick, P., Bogusch, S., Feistel, K., Blum, M., 2007. Cilia-driven leftward flow determines laterality in *Xenopus*. Curr. Biol. 17, 60–66.

Shiratori, H., Hamada, H., 2006. The left–right axis in the mouse: from origin to morphology. Development 133, 2095–2104.

Sive, H.L., Grainger, R.M., Harland, R.M., 2000. Early Development of *Xenopus laevis*: A Laboratory Manual. Cold Spring Harbor Laboratory Press, Cold Spring Harbor, NY.

Sun, Z., Amsterdam, A., Pazour, G.J., Cole, D.G., Miller, M.S., Hopkins, N., 2004. A genetic screen in zebrafish identifies cilia genes as a principal cause of cystic kidney. Development 131, 4085–4093.

Sutters, M., Germino, G.G., 2003. Autosomal dominant polycystic kidney disease: molecular genetics and pathophysiology. J. Lab. Clin. Med. 141, 91–101.

Veizis, E.I., Carlin, C.R., Cotton, C.U., 2004. Decreased amiloride-sensitive Na+ absorption in collecting duct principal cells isolated from BPK ARPKD mice. Am. J. Physiol.: Renal Physiol. 286, F244–F254.

Vignali, R., Poggi, L., Madeddu, F., Barsacchi, G., 2000. HNF1(beta) is required for mesoderm induction in the *Xenopus* embryo. Development 127, 1455–1465.

Vize, P.D., 2003. The chloride conductance channel ClC-K is a specific marker for the *Xenopus* pronephric distal tubule and duct. Gene Expr. Patterns 3, 347–350.

Vize, P., Woolf, A., Bard, J., 2002. The Kidney: From Normal Development to Congenital Diseases. Academic Press, San Diego.

Vize, P.D., Carroll, T.J., Wallingford, J.B., 2003. Induction, Development, and Physiology of the Pronephric Tubules. In: Vize, P.D., Woolf, A.S., Bard, J.B. L. (Eds.), The Kidney: From Normal Development to Congenital Disease. Academic Press, Amsterdam, pp. 19–50.

Wang, L., Eckmann, C.R., Kadyk, L.C., Wickens, M., Kimble, J., 2002. A regulatory cytoplasmic poly(A) polymerase in *Caenorhabditis elegans*. Nature 419, 312–316.

Wang, P., Pereira, F.A., Beasley, D., Zheng, H., 2003. Presenilins are required for the formation of comma- and S-shaped bodies during nephrogenesis. Development 130, 5019–5029.

Ward, C.J., Hogan, M.C., Rossetti, S., Walker, D., Sneddon, T., Wang, X., Kubly, V., Cunningham, J.M., Bacallao, R., Ishibashi, M., Milliner, D.S., Torres, V.E., Harris, P.C., 2002. The gene mutated in autosomal recessive polycystic kidney disease encodes a large, receptor-like protein. Nat. Genet. 30, 259–269.

Ward, C.J., Yuan, D., Masyuk, T.V., Wang, X., Punyashthiti, R., Whelan, S., Bacallao, R., Torra, R., LaRusso, N.F., Torres, V.E., Harris, P.C., 2003. Cellular and subcellular localization of the ARPKD protein; fibrocystin is expressed on primary cilia. Hum. Mol. Genet. 12, 2703–2710.

Wessely, O., De Robertis, E.M., 2000. The *Xenopus* homologue of Bicaudal-C is a localized maternal mRNA that can induce endoderm formation. Development 127, 2053–2062.

Wessely, O., Tran, U., Zakin, L., De Robertis, E.M., 2001. Identification and expression of the mammalian homologue of Bicaudal-C. Mech. Dev. 101, 267–270.

Wilson, P.D., 2004. Polycystic kidney disease. N. Engl. J. Med. 350, 151–164.

Yoder, B.K., Hou, X., Guay-Woodford, L.M., 2002a. The polycystic kidney disease proteins, polycystin-1, polycystin-2, polaris, and cystin, are co-localized in renal cilia. J. Am. Soc. Nephrol. 13, 2508–2516.

Yoder, B.K., Tousson, A., Millican, L., Wu, J.H., Bugg Jr., C.E., Schafer, J.A., Balkovetz, D.F., 2002b. Polaris, a protein disrupted in orpk mutant mice, is required for assembly of renal cilium. Am. J. Physiol.: Renal Physiol. 282, F541–F552.

Zhou, X., Vize, P.D., 2004. Proximo-distal specialization of epithelial transport processes within the *Xenopus* pronephric kidney tubules. Dev. Biol. 271, 322–338.

Zhou, X., Vize, P.D., 2005. Pronephric regulation of acid–base balance; coexpression of carbonic anhydrase type 2 and sodium-bicarbonate cotransporter-1 in the late distal segment. Dev. Dyn. 233, 142–144.